Ergodic Capapcity of NOMA-Based Satellite Networks with Randomly Deployed Users

Xiaojuan Yan *Student Member, IEEE*, Hailin Xiao, *Member, IEEE*, Kang An, Gan Zheng, *Senior Member, IEEE*, and Symeon Chatzinotas *Senior Member, IEEE*

***Abstract*—In this letter, we investigate the ergodic capacity of an uplink satellite network using a power-domain non-orthogonal multiple access (NOMA for simplicity) to serve users simultaneously in the consideration of random deployment of satellite users. Taking into account the deployed information of served users, we derive expression for the achievable ergodic capacity of the considered networks, where an entire link budget involving propagation loss, channel statistical prosperities, and location information is considered. Moreover, expression for ergodic capacity with OMA scheme is also derived to facilitate the performance comparison. Numerical simulation results are provided to attest the validity of theoretical results and show the vital effect of key parameters, such as the deployed information and link quality on the considered networks.**

***Index Terms*—Power-domain non-orthogonal multiple access (NOMA), satellite networks, ergodic capacity.**

I. Introduction

Satellite network will play an important role in the upcoming 5G networks in providing ubiquitous coverage for areas where terrestrial wireless infrastructures are difficult/unecnomical to be deployed, such as desert and suburban [1]. However, due to the usage of orthogonal multiple access (OMA) scheme, satellite networks provide service at an inefficiency way in terms of resource utilization efficiency, since a resource block, i.e., a time/frequency/code block, is absolutely allocated to one user [2]. Such scheme limits the number of users to be served, and further limit the ability of satellite networks to meet the demand of providing high quality of service (QoS) for a large number of users at a high resource efficiency in future satellite communications [3]. Under this condition, new multiple access schemes, which can provide an improved spectrum efficiency, high connectivity, and harmoniously integrate with the existing OMA scheme, should be considered in future satellite networks.

The authors gratefully acknowledge the support from the National Natural Science Foundation of China under Grants 61472094, 61471392, and 61261018, the UK EPSRC under grant EP/N007840/1.

X. Yan and H. Xiao (corresponding author) are with the Key Laboratory of Cognitive Radio and Information Processing (Guilin University of Electronic Technology), Ministry of Education, Guilin 541004, China, X. Yan is also with the Engineering Training Center, Qinzhou University, Qinzhou 535011, China (e-mail: yxj9609@163.com, xhl_xiaohailin@163.com).

K. An is with the 63rd Research Institute, National University of Defense Technology, Nanjing 210007, China (e-mail: ankang@nuaa.edu.cn).

G. Zheng is with the Wolfson School of Mechanical, Electrical, and Manufacturing Engineering, Loughborough University, Loughborough LE11 3TU, U.K. (e-mail: g.zheng@lboro.ac.uk).

S. Chatzinotas is with the Interdisciplinary Centre for Security, Reliability and Trust, University of Luxembourg, Luxembourg, Luxembourg (e-mail: symeon.chatzinotas@uni.lu).

Recently, a novel multiple access, named as power-domain non-orthogonal multiple access (NOMA for shortly) scheme has been proposed and viewed as one of the most promising strategies to apply in the 5G networks [4]. Since the power domain is exploited for multiple access, the NOMA can not only integrate with the existing OMA scheme, but also serve multiple users simultaneously within each resource block [5]. For these advantages, studies have been done to explore the benefit of this scheme in various networks, such as satellite networks [6–9], vehicular networks [10], and visible light communications [11]. Among the applications in satellite networks, the authors in [6] provided a comprehensive performance analysis to show the superiority of the NOMA based satellite networks. Moreover, the authors in [7] and [9] applied the NOMA scheme in downlink satellite terrestrial relay networks and cognitive satellite terrestrial networks from the perspective of providing reliable service and improving resource utilization efficiency, respectively.

However, we note that those aforementioned works [6–9] studied such benefits in the case of downlink transmission without taking the locations of NOMA users into consideration, since they were fairly relevant to users' beam gains and much challenging. To fill this gap, we investigate the performance of a NOMA based uplink satellite network, where users are randomly deployed and their locations will have impact on the system performance. Specially, a comprehensive channel model considering the locations of users is first provided. Then, based on this channel model, capacity expressions for NOMA-based and OMA-based satellite systems are derived. Finally, a set of simulation results are presented to reveal the validity of theoretical results and the vital effect of parameters, such as the location information,transmission power, and link quality on the considered system.

II. System model

Consider an uplink NOMA-based satellite system, where destinations simultaneously communicate with a satellite by applying the NOMA scheme. We assume that destinations are deployed in the same spot beam approximated as a circle of radius R. Specifically, users who are located within the disc with radius R_n, $0 \leq \mathrm{R}_n \leq \mathrm{R}$, are viewed as near users, otherwise they are viewed as far users. Moreover, users are assumed to be independent and uniformly distributed in their respective areas. As [12], the number of near and far users, i.e., N_n and N_f, are also assumed to satisfy $N_n \geq 1$ and $N_f \geq 1$, respectively. We further assume that each node in the considered system is equipped with a single antenna.

A. Channel Model

From transmission to reception, the entire link budget of User I $(I = n, f)$ can be modeled as

$$Q_I = L_I G_s(\varphi_I) G_I |g_I|^2, \quad (1)$$

where

- L_I: Free space loss (FSL) of User I is $L_I = \left(\frac{c}{4\pi f_I h_I}\right)^2$ with c, f_I, and h_I being the light speed, the frequency, and the distance from User I to satellite, respectively. Due to the fact that NOMA users are served within the same frequency and the same spot beam, we assume $L_n = L_f = L$ in this paper for simplicity.
- $G_s(\varphi_I)$: Letting φ_I, $\varphi_I = arctan(d_I/h)$ with d_I denoting the distance from beam center to User I, stand the angle between User I and beam center with respect to the satellite, the beam gain of User I is [13]

$$G_s(\varphi_I) = G_{\max}\left(\frac{J_1(u_I)}{2u_I} + 36\frac{J_3(u_I)}{u_I^3}\right)^2, \quad (2)$$

where $G_{\max}$ is the maximum antenna gain at satellite, $J_n(\cdot)$ is the Bessel function of first kind and n-th order [14], and $u_I = 2.07123 \sin\varphi_I / \sin\varphi_{I3\text{dB}}$ with $\varphi_{I3\text{dB}}$ is the beam's 3dB angle, which can be written as $\varphi_{I3\text{dB}} = arctan(R/h)$. For $h \gg R$ and $h \gg d_I$, u_I can be expressed as [15]

$$u_I \approx 2.07123 \cdot d_I/R = a d_I, \quad (3)$$

and then, (2) can be approximated by

$$G_s(\varphi_I) \approx G_{\max}\left(\frac{J_1(ad_I)}{2ad_I} + 36\frac{J_3(ad_I)}{a^3 d_I^3}\right)^2 = G_s(d_I). \quad (4)$$

The impact of the distance d_I on the $b(d_I)$, where $b(d_I) = G_s(d_I)/G_{\max}$, is plotted in Fig. 1, from which we can find that $b(d_I)$ decreases with d_I. And thus, we get that $G_s(d_n) \geq G_s(d_f)$ because of $d_n \leq d_f \leq R$.
- G_I: The the antenna gain at User I. For simplicity, $G_n = G_f$ is considered in the rest of this letter.
- $|g_I|^2$: Channel power gain of link User $I \rightarrow$satellite is assumed to follow a Shadowed-Rician fading model, which is mathematically-tractable and suitable for fixed/mobile terminals. The probability density function (PDF) of $|g_I|^2$ is given by [16]

$$f_{|g_I|^2}(x) = \alpha_I e^{-\beta_I x} {}_1F_1(m_I; 1; \delta_I x), \quad (5)$$

where $\alpha_I = \frac{(2b_I m_I)^{m_I}}{2b_I(2b_I m_I + \Omega_I)^{m_I}}$, $\delta_I = \frac{\Omega_I}{2b_I(2b_I m_I + \Omega_I)}$, $\beta_I = \frac{1}{2b_I}$ with $2b_I$ and Ω_I being the average power of the multipath and the LoS components, respectively, m_I $(m_I > 0)$ denoting the Nakagami-m fading parameter, and ${}_1F_1(a; b; c)$ representing the confluent hypergeometric function [14, Eq. (9.100)]. As [6–9], we assume that User n experiences a better fading propagation than that of User f, namely, $|g_n|^2 \geq |g_f|^2$.

Based on aforementioned assumptions, we can conclude that the link budget of the entire transmission for User n is smaller than that of User f, namely, $L_n G_s(d_n) G_n |g_n|^2 \geq L_f G_s(d_f) G_f |g_f|^2$.

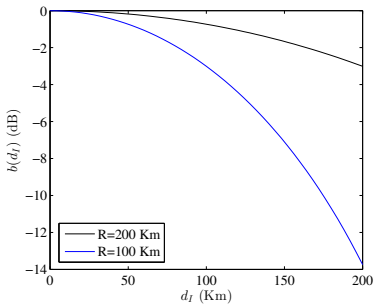

Fig. 1. $b(\varphi_I)$ versus with distance d_I.

B. signal models

1) OMA: For the OMA scheme, such as a time domain multiple access (TDMA) scheme commonly applied in satellite networks, a unit energy signal, x_I, is transmitted from User I with a transmission power, P_{I}, to the satellite in different time slots. The received signal-to-interference-plus-noise ratio (SINR) of User I is

$$\gamma_I^{\text{T}} = P_I L_I G_s(\varphi_I) G_I |g_I|^2 = \Theta_I G_s(\varphi_I) |g_I|^2, \quad (6)$$

where $\Theta_I = P_I L_I G_I$.

2) NOMA: For the uplink NOMA scheme, Users simultaneously transmit to the satellite over the same time/radio block, with their maximum or controlled transmission power. In this paper, a near and a far user are random selected from their corresponding areas to form a NOMA group. So, a superposed signal is received at the satellite and successive interference cancellation (SIC) strategy is adopted to detect each information.

Specially, User n, which has a good channel link quality and stronger at the satellite, is decoded firstly and directly, While User f must be decoded by applying the SIC strategy, which means that the signal of User f is detected after subtracting the signal of User n, x_n, from the received information. Thus, the achievable SINRs of User n and User f can be respectively derived as

$$\gamma_n^{\text{N}} = \frac{\Theta_n G_s(\varphi_n) |g_n|^2}{\Theta_f G_s(\varphi_f) |g_f|^2 + 1}, \quad (7)$$

and

$$\gamma_f^{\text{N}} = \Theta_f G_s(\varphi_f) |g_f|^2. \quad (8)$$

III. Ergodic Capacity

The ergodic capacities for both NOMA-based and OMA-based uplink satellite networks are analyzed as follows:

A. OMA

The ergodic capacity with the TDMA scheme is

$$\begin{aligned} C^T =& \ 0.5E\left[\log\left(1+\gamma_n^T\right)\right] + 0.5E\left[\log\left(1+\gamma_f^T\right)\right] \\ =& \ 0.5\int_0^{\text{R}_n}\int_0^{\infty} \log\left(1+\gamma_n^T\right) f_{|g_n|^2}(x) f_{d_n}(y)\, dxdy \\ &+0.5\int_{\text{R}_n}^{\text{R}}\int_0^{\infty} \log\left(1+\gamma_f^T\right) f_{|g_f|^2}(x) f_{d_f}(y)\, dxdy, \quad (9) \end{aligned}$$

where factor 0.5 appears owing to the time resources needed with the TDMA scheme are twice of that with the NOMA scheme. Moreover, the location PDFs of User n and User f can be respectively given by

$$f_{d_n}(y) = \frac{2\pi y}{\pi R_n^2}, \tag{10}$$

and

$$f_{d_f}(y) = \frac{2\pi y}{\pi (R^2 - R_n^2)}. \tag{11}$$

To evaluate (9), we express ${}_1F_1(m_I; 1; \delta_I x)$ in (5) and $\log(1+x)$ into series with [14, Eq. (9.14.1)] and Meijer-G functions with [14, Eq. (?)], as

$${}_1F_1(m_I; 1; \delta_I x) = \mathrm{e}^{\delta_I x} \sum_{k=0}^{m_I-1} \frac{(-1)^k (1-m_I)_k \delta_I^k}{(k!)^2} x^k, \tag{12}$$

and

$$\log(1+x) = \frac{1}{\ln 2} G_{2,2}^{1,2}\left[x \left| \begin{array}{c} 1,1 \\ 1,0 \end{array} \right. \right], \tag{13}$$

with $(x)_k$ and $G_{2,2}^{1,2}[\cdot|\cdot]$ being the Pochhammer symbol [14, p.xliii] and the Meijer-G function [14, Eq. (9.301)], respectively. Then, substituting (2), (5), (12), and (13) into (10) along with the help of [14. 7.813.1], we obtain the result as given in (14).

B. NOMA

The ergodic capacity of the considered system with the NOMA scheme can be written as

$$C^N = E\left[\log\left(1+\gamma_n^N\right)\right] + E\left[\log\left(1+\gamma_f^N\right)\right]. \tag{15}$$

Substituting (7) and (8) into (15) along with some manipulations, we have

$$C^N = E\left[\log\left(1+\Theta_f G_s(\varphi_f)|g_f|^2 + \Theta_n G_s(\varphi_n)|g_n|^2\right)\right]. \tag{16}$$

Since the expression for the PDF of $\Theta_f G_s(\varphi_f)|g_f|^2 + \Theta_n G_s(\varphi_n)|g_n|^2$ is unavailable, C^N cannot be derived directly.

TABLE I
PARAMETERS INVOLVED IN FADING MODEL [11].

Shadowing	b_I	m_I	Ω_I
Infrequent light shadowing (ILS)	0.158	19.4	1.29
Average shadowing (AS)	0.126	10.1	0.835
Frequent heavy shadowing (FHS)	0.063	0.739	8.97×10^{-4}

To conquer this difficult, we apply the results reported in [3] and hence consider the tight lower bound for (16) as

$$C_L^N = \log\left(1+e^{E\left[\ln\left(\Theta_n G_s(\varphi_n)|g_n|^2\right)\right]} + e^{E\left[\ln\left(\Theta_f G_s(\varphi_f)|g_f|^2\right)\right]}\right). \tag{17}$$

By defining I_1 and I_2 to denote the first argument and second argument in (17), substituting (4), (5), and (10)–(12) into (17), and applying [14, Eq.(4.352.1)], I_1 and I_2 can be derived as (18) and (19), respectively. Then, pulling (18) and (19) into (17), the lower bound of C_L^N can be obtained.

IV. NUMERICAL RESULTS

In this section, numerical results are provided to demonstrate the impact of key parameters on the ergodic capacity. Specifically, the parameters involved in various shadowing scenarios are given in Tab. 1 [16]. In this situation, we consider the carrier frequency as 1.6 GHz, $R = 120$ Km, FSL as $L = 154$ dB, $G_n = G_f = 3.5$ dBi, and $G_{\max} = 24.3$ dBi [17]. Moreover, The label AS/FHS presents the link shadowing severity of User n/User f.

We first conduct numerical simulations to compare the ergodic sum capacity of two multiple access schemes and validate our theoretical analysis, as depicted in Fig. 2, where $P_n = P_f = 10$ dBm, $R_n = 20$ Km, and $R_f = R - R_n$ are considered. It can be observed that capacity curves of two schemes all degrade with R_f, which reveals that the sum capacity performance is closely related to the deployment information of User f. Meanwhile, the capacity curves with the NOMA schemes over those with the TDMA schemes in all cases, demonstrating the advantages of employing the NOMA scheme in the uplink satellite networks. Specially, we note that the ascendancy of the NOMA scheme is improved when

$$\begin{aligned} C^T = &\frac{\alpha_n}{\ln 2} \sum_{k=0}^{m_n-1} \frac{(-1)^k (1-m_n)_k \delta_n^k}{\pi R_n^2 (k!)^2 (\beta_n - \delta_n)^{k+1}} \int_0^{R_n} G_{3,2}^{1,3}\left[\frac{\Theta_n G_s(y)}{\beta_n - \delta_n} \left| \begin{array}{c} -k,1,1 \\ 1,0 \end{array} \right. \right] y dy \\ &+ \frac{\alpha_f}{\ln 2} \sum_{k=0}^{m_f-1} \frac{(-1)^k (1-m_f)_k \delta_f^k}{\pi (R^2 - R_n^2)(k!)^2 (\beta_f - \delta_f)^{k+1}} \int_{R_n}^{R} G_{3,2}^{1,3}\left[\frac{\Theta_f G_s(y)}{\beta_f - \delta_f} \left| \begin{array}{c} -k,1,1 \\ 1,0 \end{array} \right. \right] y dy, \end{aligned} \tag{14}$$

$$I_1 = \ln \Theta_n G_{\max} + \alpha_n \sum_{k=0}^{m_n-1} \frac{(-1)^k (1-m_n)_k \delta_n^k}{k! (\beta_n - \delta_n)^{k+1}} \left[\psi(k+1) - \ln(\beta_n - \delta_n)\right] + \frac{4}{R_n^2} \int_0^{R_n} \ln\left(\frac{J_1(ax)}{2ax} + 36 \frac{J_3(ax)}{a^3 x^3} \right) x dx. \tag{18}$$

$$I_2 = \ln \Theta_f G_{\max} + \alpha_f \sum_{k=0}^{m_f-1} \frac{(-1)^k (1-m_f)_k \delta_f^k}{k! (\beta_f - \delta_f)^{k+1}} \left[\psi(k+1) - \ln(\beta_f - \delta_f)\right] + 4 \int_{R_n}^{R} \ln\left(\frac{J_1(ax)}{2ax} + 36 \frac{J_3(ax)}{a^3 x^3} \right) \frac{x}{R^2 - R_n^2} dx. \tag{19}$$

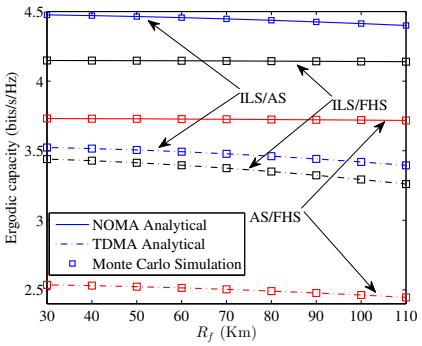

Fig. 2. Ergodic capacity of the considered system versus R_f with different fading scenarios.

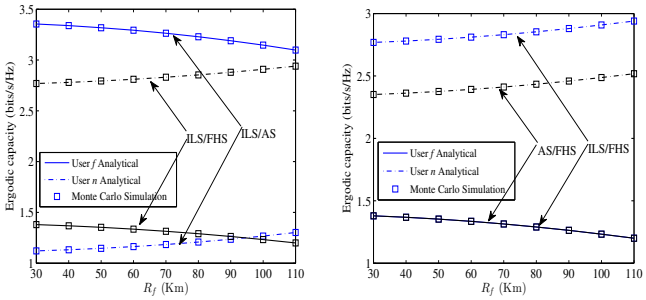

(a) (b)

Fig. 3. Ergodic capacity versus R_f with various shadowing scenarios: (a) Various fading severities of User f and (b) Various fading severities of User n.

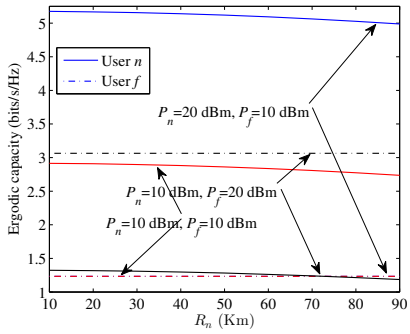

Fig. 4. Ergodic capacity versus R_n for each user with different transmission powers.

the link quality of User f or User n improves, which consist with the analytical result given in (16). Moreover, it can be observed that the analytical results are all in agreement with the Monte Carlo simulations.

Then, we analyze the effect of shadowing severity on capacity performance. The impact of fading severity of User f on users' performance is depicted in Fig. 3(a), from which we can find that the fading severity of User f has a directly impact on the performance of User n, i.e., a better link condition of User f can obviously enhance the capacity performance of User f, but simultaneously degrade the performance of User n. However, as observed in Fig. 3(b), the fading severity of User n has no impact on the performance of User f. The reason behind these phenomenons is that User n experiences interference from User f, but User f receives zero interference from User n, as γ_n^{N} and γ_f^{N} given in (7) and (8), respectively.

The effects of transmission power and location information of User n on users' performance are illustrated in Fig. 4, where ILS/HS and $R_f = 100$ Km are considered. As seen in this figure, R_n has no bearing on the capacity performance of User f, but has an effect on the performance of User n. Moreover, it can be observed that capacity curves of User n degrades when P_n decreases or P_f increases, implying that besides the location information and link condition, transmission power must be taken into account to adjust users' capacity performance.

V. CONCLUSIONS

In this letter, we have studied the capacity performance of a NOMA-based satellite networks with randomly deployed users. Specially, based on the channel model which takes the location information of users into account, we have derived expressions for ergodic capacity of the considered system. Then, simulations have been provided to show the impact of the location information, transmission power, and link quality on the considered system.

REFERENCES

[1] L. Kuang, X. Chen, C. Jiang, H. Zhang, and S. Wu, "Radio resource management in future terrestrial-satellite communication networks," *IEEE Wireless Commun.*, vol. 24, no. 5, pp. 81–87, Oct. 2017.

[2] Y. Cai *et al.*, "Modulation and multiple access for 5G networks," *IEEE Commun. Surv. Tut.,*, vol. 20, no. 1, pp. 629–646, Oct. 2017.

[3] K. An, M. Lin, and T. Liang, "On the performance of multiuser hybrid satellite terrestrial relay networks with opportunistic scheduling," *IEEE Commun. Lett.*, vol. 19, no. 10, pp. 1722–1725, Oct. 2015.

[4] Y. Saito, Y. Kishiyama, A. Benjebbour, T. Nakamura, and A. Li, K. Higuchi, "Non-orthogonal multiple access (NOMA) for cellular future radio access," in *Proc. VTC'13*, Dresden, Germany, Jun. 2013, pp. 1–5.

[5] Z. Ding *et al.*, "Cooperative non-orthogonal multiple access in 5G systems," *IEEE Commun. Lett.*, vol. 19, no. 8, pp. 1462–1465, Aug. 2015.

[6] X. Yan, H. Xiao, C.-X. Wang, K. An, A. T. Chronopoulos, and G. Zheng, "Performance analysis of NOMA-based land mobile satellite networks," *Proc. IEEE ACCESS*, Vol. 6, pp. 31327–31339, Jun. 2018.

[7] X. Yan *et al.*, "Hybrid Satellite Terrestrial Relay Networks with Cooperative Non-Orthogonal Multiple Access," *IEEE Commun. Lett.*, vol. 22, no. 5, pp. 978–981, May 2018.

[8] X. Yan *et al.*, "Outage performance of NOMA-based hybrid satellite-terrestrial relay networks," *IEEE Wireless Commun. Lett.*, in press.

[9] X. Yan *et al.*, "On the ergodic capacity of NOMA-based cognitive hybrid satellite terrestrial networks," *Proc. IEEE ICCC*, Oct. 2017.

[10] B. Di *et al.*, "V2X meets NOMA: non-orthogonal multiple access for 5G-enabled vehicular networks," *IEEE Wireless Commun.*, vol. 24, no. 56, pp. 14–21, Dec. 2017.

[11] X. Zhang *et al.*, "User grouping and power allocation for NOMA visible light communication multi-cell networks," *IEEE Commun. Lett.*, vol. 21, no. 4, pp. 777–780, Apr. 2017.

[12] Y. Liu *et al.*, "Cooperative non-orthogonal multiple access with simultaneous wireless information and power transfer," *IEEE J. Sel. Areas Commun.*, vol. 34, no. 4, pp. 938–953, Apr. 2016.

[13] G. Zheng, S. Chatzinotas and B. Ottersten, "Generic optimization of linear precoding in multibeam satellite systems," *IEEE Trans. Wireless Commun.*, vol. 11, no. 6, pp. 2308–2320, June 2012.

[14] I. S. Gradshteyn and I. M. Ryzhik, *Table of Integrals, Series, and Products*, 7th ed. New York, NY, USA: Academic, 2007.

[15] J. Arnau *et al.*, "Performance of the multibeam satellite return link with correlated rain attenuation," *IEEE Trans. Wireless Commun.*, vol. 13, no. 11, pp. 6286–6299, Nov. 2014.

[16] A. Abdi, W. Lau, M.-S. Alouini, and M. Kaveh, "A new simple model for land mobile satellite channels: first and second order statistics," *IEEE Trans. Wireless. Commun.*, vol. 2, no. 3, pp. 519–528, May 2003.

[17] G. Zheng, S. Chatzinotas and B. Ottersten, "Generic optimization of linear precoding in multibeam satellite systems," *IEEE Trans. Wireless Commun.*, vol. 11, no. 6, pp. 2308–2320, June 2012.